Smoluchowski Coagulation Models Of Sea Ice Thickness Distribution Dynamics

D. Godlovitch,[1] R. Illner,[2] and A. Monahan,[1]

D. Godlovitch, School Of Earth And Ocean Science, University Of Victoria, 3800 Finnerty Road Victoria BC, V8N 1M5 (dgodlovi@uvic.ca)

R. Illner, Department of Mathematics and Statistics, University Of Victoria, 3800 Finnerty Road Victoria BC, V8P 5C2

A. Monahan, School Of Earth And Ocean Science, University Of Victoria, 3800 Finnerty Road Victoria BC, V8N 1M5

[1] School Of Earth And Ocean Science,
University Of Victoria, Victoria, BC, Canada

[2]Department of Mathematics and Statistics,
University Of Victoria, Victoria, BC, Canada

Abstract. Sea ice thickness distributions display a ubiquitous exponential decrease with thickness. This tail characterises the range of ice thickness produced by mechanical redistribution of ice through the process of ridging, rafting, and shearing. We investigate how well the thickness distribution can be simulated by representing mechanical redistribution as a generalized stacking process. Such processes are naturally described by a well-studied class of models known as Smoluchowski Coagulation models, which describe the dynamics of a population of fixed-mass ”particles” which combine in pairs to form a ”particle” with the combined mass of the constituent pair at a rate which depends on the mass of the interacting particles. Like observed sea ice thickness distributions, the mass distribution of the populations generated by SCMs has an exponential or quasi-exponential form. We use SCMs to model sea ice, identifying mass-increasing particle combinations with thickness-increasing ice redistribution processes. Our model couples an SCM component with a thermodynamic component and generates qualitatively accurate thickness distributions with a variety of rate kernels. Our results suggest that the exponential tail of the sea ice thickness distribution arises from the nature of the ridging process, rather than specific physical properties of sea ice or the spatial arrangement of floes, and that the relative strengths of the dynamic and thermodynamic processes are key in accurately simulating the rate at which the sea ice thickness tail drops off with thickness.

1. Introduction

The sea ice found in the polar oceans plays a major role in the Earth's climate due to its high albedo and insulating properties. Inclusion of a dynamic sea-ice component in General Circulation Models (GCMs) is essential in accurate predictions of climactic behaviour, and the sensitivity of a GCM's output to its sea-ice component has been well studied (*e.g.*, Bitz et al. [2001], Holland et al. [2006]). Among the most difficult aspects of modelling sea-ice is the inclusion of the processes which create thick ice through the compressive fracture and piling of floes. Due to the complex nature of the interactions between ice floes and the many spatial scales at which this activity occurs, modelling sea-ice dynamics presents many challenges.

Observations of sea ice indicate that population statistics often follow well defined distributions. Perhaps the best known is the tendency of the ice thicknesses to follow an exponential distribution above approximately 2 meters Wadhams and Davy [1986]. Additionally, as described in the work of Lensu Lensu [2003], the distance between ridges is approximately log-normally distributed. Aerial measurements have revealed that the area of individual floes in a sea ice population also follows a log-normal distribution. Given that all of these statistical properties of the sea ice population are a result of the redistribution process, a measure of the success of a model of sea ice should be its ability to reproduce them. Any multi-year simulations which include a sea ice component will require accurate representation of the sea ice's extent and concentration from year to year, and accurate modelling of the thickness distribution is necessary in determining the inter-annual behaviour of a population of sea ice, as it is the thickest ice which is most likely to survive a summer melt period.

45

46 A typical example of a sea ice thickness distribution is seen in Fig. 1, which displays the
47 mean population thickness distribution obtained from multi-year sea ice thickness data taken in
48 the Beaufort Sea (on semilog axes, the exponential tail is linear). Further examples of observa-
49 tions of exponentially distributed populations may be seen in, the work of Wadhams (Wadhams
50 [1983], Wadhams [1987]). The scaling constant of the distribution varies with time of year
51 and geographical location. An exponential distribution does not accurately describe the entire
52 population: the thinner ice, typically below 2 meters, deviates sharply from an exponential dis-
53 tribution (Fig. 1). For this range of thicknesses the population dynamics are dominated by the
54 thermodynamic processes. The ubiquity of the exponential tail in thicker ice strongly suggests
55 that it arises as the consequence of some generic feature of the physical properties of the system,
56 and is not due to a specific temperature regime, or a region-specific pattern in the atmospheric
57 and oceanic forces acting upon the ice.

58

59 Although the exponential form of the thickness distribution is well documented, the exact
60 mechanisms responsible for this feature of sea-ice populations have not been fully explored.
61 Most previous work on sea ice dynamics has focused on large-scale simulations using force
62 balance models with complex redistribution dynamics (*e.g.*, Feltham [2008],Hibler [2001]).
63 Early force-balance models were unable to capture the details of the dynamics of the thickness
64 distribution due to having a small number of thickness categories. For example, the original
65 Hibler model Hibler [1979] only had two thickness categories. Variable thickness models de-
66 rived from Hibler's basin scale model (Hibler [1980], Flato and Hibler [1995]), produce a more
67 realistic thickness distribution, although they typically overestimate the proportion of the pop-

ulation of thick ice. Aside from a proof-of-concept model by Thorndike Thorndike [2000], in which the merits of a more conceptual approach were suggested, the task of identifying the essential features of the dynamics which yield the exponential distribution has not been addressed in detail. Work using a stochastic formulation to examine the statistics of ridge spacing in ice pack has been done Lensu [2003], but the parameterisation of the ridging processes were highly abstracted, and this work does not provide a direct answer to the question of which essential features of redistribution produce the exponential tail.

Another statistic of sea ice populations which has been studied is the distribution of floe areas Rothrock and Thorndike [1984]. Analysis of observations suggests that the floe size distribution follows a power law. The result is unsurprising when the process of floe fragmentation is compared to that of the fragmentation behaviour of brittle solids. The fragment size distribution resulting from the fracture of brittle material has been found to take a power law distribution, with the value of the exponent depending upon the material Turcotte [1986]. The power laws used to describe the size distributions of fragments possess the characteristic property of self-similarity or scale-invariance. This self similarity is vividly illustrated in the visual similarity of images of sea ice taken at widely-separated scales (e.g.Rothrock and Thorndike [1984]).

Our approach to studying the relationship between the redistribution process and the evolution of the thickness distribution will make use of an idealised representation of redistribution. Rather than try to create a model which captures the full complexity of the redistribution process, we will instead represent ice-ice interactions as the simple process of stacking of floes on top of one another. This approach to modelling the thickness distribution dynamics allows us to

assess whether the ubiquitous exponential tails are a result of the detailed material properties of sea ice or simply of the process of stacking.

We consider a population of floes of equal size and of fixed thickness, occupying an area A. We define the thickness distribution $g(h)$ such that $g(h)\mathrm{d}h$ is the fraction of the area A occupied by floes of thickness h. Open water is represented by floes of thickness zero. The dynamic interactions between floes are represented as a stacking process which combines a floe of thickness h_1 with a floe of thickness h_2 to create a single floe of thickness $h_1 + h_2$. We make the simplifying "mean-field" assumption that any two floes in the domain may interact. The fraction of the region A which was occupied by the two floes is now occupied by the stacked floe of thickness $h_1 + h_2$ and a floe of thickness zero (open water). As will be detailed in Section 4, while a floe of thickness zero effectively does not participate in dynamics of the stacking process, the inclusion of a thermodynamic component of the model which grows and melts the ice towards a seasonal equilibrium means that open water is a source of new thin ice during the growth season which will then be available to participate in the stacking process.

The representation in our model of the ice redistribution process as one of stacking is inspired by the dynamics of Smoluchowski Coagulation Models (SCMs), which are natural tools for studying the relationship between the physical processes that drive the evolution of populations of ice and their statistical features. In its simplest form, the SCM is a system of ordinary differential equations describing the dynamics of a population of individual elements (usually referred to as 'particles') defined by their 'mass' which can interact with each other by combining to form larger particles. The SCM paradigm can be naturally extended to include fragmentation

processes, wherein a particle dissociates into two smaller particles. Having demonstrated their utility as a tool in statistical mechanics, SCMs are a well-studied family of equations which admit analytical solutions in some instances. Such models are potentially of great use for the study of sea ice populations, in particular providing insight regarding the parameterisations of thickness redistribution processes in sea ice components of GCMs.

In this paper we first provide a brief overview of the behaviour of SCMs (Section 2). We then examine an earlier model of sea ice thickness dynamics Thorndike [2000] which represents the redistribution as a special case of an SCM (Section 3). To provide an illustration of the potential that the SCM formulation shows in sea-ice modelling, we then demonstrate how a simple SCM model of sea ice thickness distribution dynamics captures the essential features of the thickness distribution tail independent of the parameterisation of the stacking process rate (Section 4). This model is not strictly an SCM, but augments an SCM core representation of redistribution with parameterisations of thermodynamic processes and open water formation. An extension of these results to the distribution of floe sizes is presented in Section 6, followed by a discussion and conclusions in Section 7.

2. Smoluchowski Coagulation Models

The SCM was derived in the early 20th century and describes the dynamics of a population of particles of varying mass which may combine with each other (coagulate) in pairs to form more massive particles. First used to describe statistical mechanical processes in gases, the coagulation model has been extensively studied and has demonstrated utility in a variety of areas in applied mathematics, ranging from astronomy to population genetics. While it is possible to describe the type of system for which the SCM was developed using a model which includes

spatial information, for the purposes of simplicity and tractability, the SCM does not include the location or velocity of individual particles. Instead, the rate of combinations of particles of masses x and y is determined by the number of particles of each mass and the masses of the particles.

Particle masses may be discrete or continuous. The interaction rule states that two particles of mass x and y may interact ('coagulate') to create a single particle of mass $x + y$. In the case where the particle masses are discrete, they may be enumerated by the natural numbers. We may write a set of functions, $u_k(t)$, the k^{th} element of which gives the number of particles of mass k at time t. We may then write the set of coupled differential equations for the discrete SCM:

$$\frac{\mathrm{d}u_k(t)}{\mathrm{d}t} = \frac{1}{2}\sum_{j=1}^{k-1} K(k-j,j)u_j(t)u_{k-j}(t) - u_k(t)\sum_{j=1}^{\infty} K(j,k)u_j(t). \tag{1}$$

The k^{th} equation describes the time rate of change of the number of particles of mass k. The first term on the right hand side is a source term, which accounts for all possible ways to make particles of mass k by combining particles of mass j and $k - j$. The second term on the right is the sink term, covering all of the possible combinations that a particle of mass k may make with other particles.The rate at which interactions occur is determined by a kernel $K(x, y)$, which encodes the detailed physical behaviour of the "particles" in the system. The kernel is a representation of the spatially-averaged microscopic dynamics of the system under study. A detailed example of the derivation of a kernel from specific microscopic physics is found in Hammond et al. [2007]. The kernel K should be symmetric in its arguments, as it is assumed that the only factor which affects the rate at which particle interactions occur (besides the particle number) is their mass. The symmetry of K requires the insertion of a factor of $1/2$ before the source

158 term in order to avoid double-counting of interactions. Examples of SCM kernels arising from
159 particular physical problems may be found in Aldous [1999].

160

161 The continuous analogue of Eqn. 1 uses a single function $u(x,t)$ to describe the number density
162 of the population, with dynamics described by the integro-differential equation:

$$\frac{\partial}{\partial t}u(x,t) = C(u) \tag{2}$$

163 where

$$C(u) = \frac{1}{2}\int_0^x K(x-x',x')u(x',t)u(x-x',t)\mathrm{d}x' - u(x,t)\int_0^\infty K(x',x)u(x',t)\mathrm{d}x'. \tag{3}$$

164 As with the discrete equation, the first term on the right hand side is the source term, the second
165 is the sink term, and $K(x,x')$ is a symmetric rate kernel.

2.1. Analytic Solutions

166 The appeal of developing a model of sea ice thickness dynamics based on the SCM formula-
167 tion is its simplicity and universality. It is a generic representation of a system in which smaller
168 elements combine to form larger ones. A variety of physical systems may be modelled by
169 choosing the appropriate kernel. Although the system is inherently non-linear, there are some
170 kernels for which it admits a simple analytic solution given initial conditions in which all par-
171 ticles are of a single mass ($u_{k^*}(0) = M$ for $k = k^*$, and zero otherwise in the discrete case; and
172 $u(x,0) = \delta(x_0)$ for some x_0 in the continuous case) Aldous [1999].

173

174 For a range of analytic forms of $K(x,y)$ for which analytic solutions can be determined, these
175 solutions (discussed in detail the Appendix) are approximately exponential in form. That these
176 near-exponential populations arise from SCMs with a variety of rate kernels suggests that the

robustness of the exponential tail of sea ice thickness may simply be a consequence of the redistribution dynamics naturally being expressed as such a model.

It is important to note that SCMs conserve mass but not the population size, and the total number of particles decreases with time as they coalesce. The SCM framework may be suitable to describe the way process of ice redistribution form ridge structures, but it does not include the relevant process of the formation of open water through the dilation of the pack which can accompany redistribution, or thermodynamic ice thickness evolution. The nature of the dynamics described by SCMs precludes the possibility of the creation of particles in the lowest mass category and the decrease in the total number of particles results from the lack of any source terms for particles of the smallest mass in either Eqn. 1 or Eqn. 2. For this reason, the SCM on its own cannot provide a complete description of the dynamics of the normalized sea ice thickness distribution, and we must consider additional terms, as will be discussed in Section 3.

To further illustrate the connection between the solutions of SCMs and exponential distributions, we can consider the statistical features of the population dynamics described by constant coagulation kernel SCMs. It was already noted that as a result of the steady decrease in the number of particles in the population, we cannot interpret u_k as a probability distribution. However, we may look at the distribution at a particular time by normalising each $u_k(t)$ by the total number of particles at that time. With a constant coagulation kernel, differential equations for the moments of the distribution of particle masses at time $t = t_*$ may be derived, and their asymptotic behaviour analysed Frenklach [1985]. The moments about zero of the probability

distribution arising as a solution may be written as

$$\mu'_n(t) = \frac{m_n(t)}{m_0(t)}. \tag{4}$$

with $m_r(t) = \sum_k k^r u_k(t)$. When $K = 1$ in Eqn.1 the time evolution of the $m_k(t)$ is given by:

$$\frac{\mathrm{d}}{\mathrm{d}t} m_0(t) = -\frac{1}{2} m_0^2 \tag{5}$$

$$\frac{\mathrm{d}}{\mathrm{d}t} m_1(t) = 0 \tag{6}$$

$$\frac{\mathrm{d}}{\mathrm{d}t} m_k(t) = \frac{1}{2} \sum_{j=1}^{k-1} \binom{k}{j} m_j(t) m_{k-j}(t) \quad k > 1. \tag{7}$$

These equations may be solved given a set of initial conditions $\{m_{i,0}\}$. One may write expressions for the $m_k(t)$ in terms of these initial conditions,

$$m_0(t) = (1 + t/2)^{-1}$$

$$m_1(t) = m_{1,0}$$

$$m_2(t) = m_{2,0} + m_{1,0}^2 t$$

$$m_3(t) = m_{3,0} + 3m_{2,0}t + 3t^2/2$$

The moments about zero, μ'_k may be then be calculated from the $m_k(t)$. From these terms, the moments of the the mass distribution at a particular time may be calculated: the mean is given by $\mu = \mu'_1$, the variance by $\sigma^2 = \mu'_2 - (\mu'_1)^2$, and so on. With the initial condition that the entire population is comprised of particles of the smallest mass, $m_{i,0} = 1$, we may obtain expressions for the moments of the distribution which tend asymptotically towards those of the exponential distribution Frenklach [1985]. Furthermore, it is possible to estimate the rates of convergence of the system's moments. These exact results require the initial conditions to have all particles concentrated in the lowest thickness category, which makes the description of convergence to

an exponential distribution analogous to descriptions of the growth by redistribution processes of a population of ice in a region that is ice-free in the summer, and consequently populated by level ice of a single thickness at the start of the growth season.

3. A Case Study: Thorndike's Pseudo-SCM

An idealised model exploring the dynamics of the sea ice thickness distribution $g(h)$ under the combined action of ridging and thermodynamic forcing was introduced by Thorndike Thorndike [2000]. This model demonstrates that the exponential tail of $g(h)$ arises in a simple system that assumes a fixed population of ice 'particles', each of a certain thickness. An ice particle of thickness x 'ridges' with a particle of thickness y to create a particle of thickness $x + y$ and one of thickness 0 (open water). This formulation is extremely similar to an SCM, although this connection was not made in Thorndike [2000]. Thorndike's model differs from an SCM only in the addition of the δ function term to create ice of thickness zero (open water), and in the inclusion of a representation of thermodynamically driven growth and melt.

Mathematically, Thorndike's system may be written

$$\frac{\partial g}{\partial t} = -\frac{\partial (fg)}{\partial h} + r\left[\delta(h) - 2g(h) + \int_0^h g(h')g(h-h')\mathrm{d}h'\right]. \tag{8}$$

The first term on the right hand is the annual average thermodynamic growth and ablation rate, given by

$$\frac{\partial (fg)}{\partial h} = F\frac{\partial (H-h)g}{\partial h}, \tag{9}$$

where H is the thermodynamic equilibrium thickness and F is a coefficient which determines the rate at which ice approaches the thermodynamic equilibrium thickness. The terms arising from ice-ice interactions are all within the square brackets. The rate of these interactions scaled

by a constant r, which is independent of the thickness of the ice involved. In the terminology of the SCM, this corresponds to a constant kernel $K(x, y) = r$. The delta function represents the creation of open water when two members of the population combine. This open water subsequently freezes over and thus acts as a source for thin ice. The integral is the source term for ice of thickness h, associated with ridging. The term $-2g(h)$ is a sink term, representing the transfer of ice of thickness h to higher thicknesses through the ridging process. This is formally identical to the sink term in the SCM with a uniform kernel, as $g(h)$ is a normalised probability distribution and so

$$\left[\int_0^\infty g(h')\mathrm{d}h'\right] g(h) = g(h). \tag{10}$$

By including the delta-function, the integral over thickness of the redistribution terms, (*i.e.*, the net effect on $g(h)$ of the redistribution process), is formally zero, *viz.*,

$$\int_0^\infty \left[\delta(h) - 2g(h) + \int_0^h g(h')g(h-h')\mathrm{d}h'\right]\mathrm{d}h = 0.$$

The thermodynamic term in Eqn. 8 also integrates to zero over h,so there is no difficulty in interpreting g(h) as a normalized probability distribution. As shown in Thorndike [2000], both approximate analytic calculations and numerical simulation demonstrate that in steady state this model predicts an exponential tail for $g(h)$.

As we have remarked, the pure SCM will not normally serve as a model of the dynamic behaviour of a probability distribution (in this case the of sea ice), as, in Eqn.2 (or Eqn.1 for the discrete case) it does not conserve the integral

$$N(t) = \int_0^\infty u(x,t)\mathrm{d}t. \tag{11}$$

As noted above, the delta function term in Thorndike's model represents the creation of open water at the same rate as redistributions are occurring, thus conserving total particle number. We can think of the populations of ice as a set of floes, each completely occupying an individual cell of a fixed grid. Redistribution is the process of removing a floe from one grid cell and adding its thickness to a floe in another cell. The difference between the redistribution processes described by the SCM and Thorndike's model may be understood as the difference between generating a thickness 'distribution' by examining only the cells occupied by ice (the SCM); and generating the population by counting all grid cells, including the ones which are occupied by open water (Thorndike's representation of redistribution). Given the success of Thorndike's model at capturing the essential features of the equilibrium thickness distribution, it is worthwhile to extend this earlier analysis using perspectives provided by the SCM.

$$\frac{\mathrm{d}g_k(t)}{\mathrm{d}t} = -\frac{\partial T g_k(t)}{\partial h} + r\left[\delta_{k,1} - 2g_k(t) + \sum_{j=1}^{k} g_j(t) g_{k-j}(t)\right]. \tag{12}$$

4. The Generalised Thorndike Model

A general model of sea ice thickness distribution evolution containing an SCM component to describe the dynamic interactions between floes can be built using similar assumptions to those Thorndike adopted. The common aspect of the SCM and Thorndike's model is the description of ridging as the combination of ice of thickness k and ice of thickness j to form ice of thickness $k + j$ at a rate dependent on k, j, and the quantity of ice of those thicknesses. The generalisation of Eqn.8 to include an arbitrary rate kernel yields is

$$\frac{\partial g(h,t)}{\partial t} = \frac{\partial T(g)}{\partial h} + C(K,t)\delta(h) +$$

$$\frac{1}{2}\int_0^x K(h', h-h')g(h', t)g(h-h', t)\mathrm{d}h' - \int_0^\infty K(h, h')g(h, t)g(h', t)\mathrm{d}h', \tag{13}$$

where $T(g)$ is a seasonally-dependent thermodynamics function that drives ice towards a cyclo-stationary equilibrium (limit cycle), at a rate dependent on the thickness (h). Generalization of the rate kernel requires the introduction of the factor $C(K, t)$ in the open water source term, in order to ensure that $g(h)$ remains normalized. We generalise the source term for the creation of ice of thickness 0 by calculating the rate at which all redistributions are occurring. With a general kernel, $K(x, y)$, the coefficient of the δ term takes the form

$$C(K, t) = \int_0^\infty \left[\int_0^\infty K(h, h')g(h, t)g(h', t)\mathrm{d}h'\right]\mathrm{d}h. \tag{14}$$

Note that when $K(x, y) = 1$, the coefficient of $\delta(h)$ in Eqn. 13 is equal to 1 (as in Eqn. 12); this follows from the normalisation of $g(h, t)$.

In specifying the rate at which the stacking process occurs, the kernel represents both the external forcing and the ice response to the forcing. In a situation where there are no wind or currents acting on a region of ice there will be no redistribution events, in which case the dynamic component of our model would be zero, *i.e.*, $K(h, h') = 0$. Similarly, if the ice was (hypothetically) strong enough to resist deformation and piling, the kernel would similarly be zero. While the two aspects of the physics of the situation are difficult to isolate from each other, the overall scale of the kernel may be considered to be related to the strength of the external forcing relative to the strength of the ice, while the derivative of the kernel, $\partial K/\partial h$ reflects the way in which the ice strength as a function of its thickness is represented. By specifying a kernel which is not a function of time, we assume an external forcing which does not change appreciably on the timescales over which $g(h)$ evolves. In our choice of the kernel, we will consider both the

functional form of K and its overall scale.

The discrete form of Eqn.13 is the system of equations

$$\frac{\partial g_k(t)}{\partial t} = U(T(g_k)) + C(K,t)\delta_{k,1} + \frac{1}{2}\sum_{j=1}^{k-1} K(k,k-j)g_j(t)g_{k-j}(t) - \sum_{j=1}^{\infty} K(k,j)g_k(t)g_j(t). \qquad (15)$$

where $g_k(t)$ is the fraction of the population of thickness class k. The function $C(K,t)$ is the discretised analogue of Eqn.14, and the thermodynamic term $U(T(g_k))$ is an upwind gradient operator acting on $T(g_k)$.

As we have already discussed, distributions with exponential tails (at least approximately) occur naturally in coagulation models over a broad range of kernel forms. For numerical implementation we will truncate the equations at some maximum thickness category, which we may choose to be sufficiently large that ice of that thickness is never created (in practice). Based on observations of thickness distribution, it is reasonable to simulate a population which does not produce ice above 20m and truncate the population at this thickness.

We numerically integrate this model using a forward finite difference scheme (Eqn. 15) with 200 thickness categories, each representing a 0.1m thickness increment:

$$g_k^{t+1} = g_k^t + \Delta t\left(U(T(g_k(t),t)) + \left(\sum_{k=2}^{\infty}\left[\sum_{j=1}^{k-1} K(k,k-j)g_j(t)g_{k-j}(t)\right]\right)\delta_{k,1} + \frac{1}{2}\sum_{j=1}^{i-1} K(k,k-j)g_j^t g_{k-j}^t - g_k^t\sum_{j=1}^{200-k} K(k,j)g_j^t\right) \qquad (16)$$

Thermodynamic forcing is represented as a simple cyclical function based on observations of sea ice growth and ablation rates Maykut and Untersteiner [1971], transferring a portion of ice in each thickness category to one or other of its neighbouring bins, depending on the thickness

306 of the ice and the season. The flux of ice in each thickness category in a single time step is given
307 by

$$T(g_k) = [S(t)W_1(k) + \{1 - S(t)\}W_2(k)]\, g_k, \tag{17}$$

308 where

$$W_1(k) = 0.1\exp(-1.7k\Delta h) - 0.01 \;\; m\; day^{-1}$$

$$W_2(k) = 0.01\exp(-0.01k\Delta h) \;\; m\; day^{-1}$$

309 where Δh is the width of each thickness category and

$$S(t) = \begin{cases} 1 - t/180 & 0 \le t < 180 \\ t/180 - 1 & 180 \le t < 360 \end{cases}.$$

310 with time t in days. The functions W_1 and W_2 are approximations of the winter and summer
311 growth curves given in Maykut and Untersteiner [1971], as illustrated in Fig. 2. Mass lost from
312 each thickness category due to thermodynamic processes is accounted for in its neighbouring
313 categories (higher thicknesses when $T(k)$ is positive and lower when it is negative). This form
314 of the thermodynamic forcing is idealised, in line with the rest of the formulation of the model.
315 By varying the strength of the thermodynamic term, the interplay between dynamic and ther-
316 modynamic forcing may be explored. For most of the model simulations which we perform, the
317 strength of the thermodynamic term relative to the redistribution terms is small, and the advance
318 and retreat of the tail of the distribution over the course of the seasonal cycle is not large.
319

5. Results

320 Our analysis of the behaviour of the model within the context of the SCM formulation re-
321 lies upon the assumption that the coagulation terms are dominant for ice thicknesses above the

thermodynamic equilibrium. Evidence to support this assumption can be seen by comparing the magnitudes of the coagulation and thermodynamic terms in Fig. 3, produced using the final timestep of a numerical simulation of Eqn. 15 with a linear kernel ($K = r(h + h')$). Because the model includes a seasonally-evolving thermodynamics component, it will never reach equilibrium, and so the thermodynamic and SCM terms will not add to exactly zero. The first plot in Fig. 3 displays the magnitudes of the SCM and thermodynamic terms at the final time step of the simulation over the entire thickness range. The second (lower) plot is a semilog plot, showing the absolute values of the two components for ice thicknesses greater than 3m. For ice thicknesses above 3m, the SCM component of the model is a minimum of two orders of magnitude larger than the thermodynamic component, rising to over 4 orders of magnitude at 20m. The large differences in the magnitude of the two components, particularly in the thicker ice where the tail forms lead us to conclude that the behaviour of the model in forming a quasi-exponential tail may be reasonably compared with (and attributed to) the behaviour of an SCM model.

Because the model is computationally efficient, we may perform a large number of numerical simulations, allowing us to thoroughly compare the predictions of this model to Thorndike's, and to examine how altering various parameters affects the model output. There are two major sensitivities to be explored: the functional form of the transfer kernel $K(k, j)$, and the strength of the thermodynamic forcing relative to that of mechanical redistribution. A variety of kernels may be tested, in order to assess the sensitivity of model predictions to this choice. From the discussion in Section 2, we do not expect that this sensitivity will be strong (for reasonable choices of kernel form). As part of our experimentation with the kernel, we investigate the inclusion of

345 a representation of the rafting process in which the ice is transferred laterally onto adjacent ice
346 without having first to be fragmented. This phenomenon occurs in thin ice, which is flexible
347 enough for rafting to be possible. In our model, we may represent rafting by specifying larger
348 values of the kernel $K(k, j)$ for the dynamics of ice below a certain thickness.

349

350 We may use the same thermodynamic routine in both the Thorndike model and our model.
351 In contrast with the focus on equilibrium solutions in Thorndike Thorndike [2000], the time-
352 dependence of the thermodynamic forcing in the present study allows us to consider evolution
353 of the thickness distribution across the seasonal cycle. In the simulations which we perform,
354 using $T(g(h))$ as defined by Eqn.17, the strength of the thermodynamic growth and melt relative
355 to the redistribution is small, and the advance and retreat of the tail of the population is not large
356 following its initial formation.

357

358 Simulations suggest that the choice of coagulation kernel has little qualitative effect on the pop-
359 ulation (Fig. 4). The set of kernels considered is presented in Table 1; note that for pure SCMs
360 the constant, additive, or multiplicative kernels admit analytic solutions. In each instance the
361 rate scaling coefficient r is adjusted so that the results of the simulation are similar in the extent
362 and slope of the exponential tail produced during the simulation.By including the additive and
363 multiplicative cases, which describe population dynamics in which larger "particles" interact at
364 a larger rate than smaller ones (unlike the dynamics of sea ice populations) we provide further
365 evidence that the addition of the thermodynamic and source terms does not alter the qualitative
366 nature of the simulated populations, and demonstrates the robustness of the quasi-exponential
367 distribution under a variety of qualitatively different representations of the redistribution pro-

cess.

We may also implement a crude representation of rafting by constructing $K(x, y)$ to take larger values for thin ice, to represent the lower energy required to cause thin ice to over-ride neighbouring floes. Using the constant coagulation kernel, we double the value of the constant for all ice thickness categories below a set thickness h_R,

$$K(x,y) = \begin{cases} 2r & h < h_R \\ r & h \geq h_R. \end{cases} \tag{18}$$

Although transfer rates of thin ice are enhanced, the quasi-exponential form of the solution is not affected (Fig. 5). The increased transfer rates of thin ice speed up the formation of the extended quasi-exponential tail, to a degree dependent upon the number of thickness categories with a higher transfer rate. Small values of the rafting index have a smaller effect on the simulation because the population of thin ice is naturally evacuated by the thermodynamic process in the model. As the population of raftable ice is depleted, the effect of the rafting terms will become less important to the evolution of the system.

The relative strengths of the thermodynamic and dynamic (SCM) terms are central in determining quantitative features of the simulated ice thickness distribution. We compare simulations with differing relative strengths of these components in Fig.6. Using the constant coagulation kernel, $K = R_T^{-1}$, we may examine the effect on simulations of varying the relative strength of the two components. The value of R_T clearly determines the slope of the tail of the population. When the thermodynamic term is relatively weak ($R_T < 1$), the coagulation component of the model dominates, and the slope of the tail becomes nearly flat. Conversely, under strong

thermodynamic forcing when $R(T) > 1$, the slope of the tail decreases. At large values of R_T ($R_T > 5$), thermodynamics dominate the simulation, producing strongly cyclical behaviour in response to the seasonal thermodynamic forcing.

6. Fragmentation And Self Similarity

In the previous section, we discussed the relationship between the SCM and Thorndike's sea ice model Thorndike [2000], and examined the utility of the SCM as a component of a model describing the evolution of the thickness distribution of a population of sea ice. While this is the main focus of our work, it is worthwhile to bring to attention another aspect of sea ice modelling in which an SCM perspective may prove useful.

Measurements show that the distribution of floe sizes typically follows a log-normal distribution Rothrock and Thorndike [1984],Hopkins [1998]. It is known that log-normal distributions have the property of self-similarity. It has also long been known that the fractile behaviour of brittle solids typically produces a population of fragments whose size follows a power law Turcotte [1986]. Systems of equations that produce self-similar solutions are of particular interest in modelling brittle fracture. Through the examination of observations of sea ice failure behaviour over a broad range of scales, it has been noted that the pressure threshold for ice failure followed a power law over 10 orders of magnitude in scale Sanderson [1988] (Eqn. 19), suggesting that the processes at work in sea ice fragmentation display self-similarity.

$$P_{fail} = C(\text{contact area})^{-s}, \tag{19}$$

where s is a constant between $1/4$ and $1/2$ Sanderson [1988].

A simple renormalised group (RNG) method of modelling brittle failure in ice was developed in Palmer and Sanderson [1991]. From this simple model it is possible to produce an estimate of the dependence on area of the failure pressure of ice, with the prediction that $s = 1/2$. More recently a model of fragmentation processes in ice which can lead to log-normal distributions of floe size was developed by Lensu Lensu [1997]. A population of ice occupying an area $N(t)$, with $N(t)f(x)$ floes of area x at time t evolves according to

$$\frac{\partial}{\partial t}N(t)f(x) = 2N(t)\int_x^1 \alpha(z)\beta(z \to x)f(z)\mathrm{d}z - N(t)\alpha(x)f(x), \tag{20}$$

where $\beta(z \to x)\mathrm{d}x$ is the probability that a floe of area z produces a floe of area x through fragmentation, and α is the rate at which floes of area x themselves fragment. Lensu assumed that $\alpha = 1$, and that fragmentation behaviour is area independent. We may then write

$$\beta(z \to x) = (1/z)\beta(x/z) \tag{21}$$

so that $\beta(x)\mathrm{d}x$ is a probability distribution defined for $x \in [0,\ 1]$.

The SCM may be expanded to include the process of spontaneous fragmentation of members of the population into smaller particles. In the continuous case, the equations describing a coagulation-fragmentation system take the form

$$\frac{\partial}{\partial t}m(x,t) = C(m) + \int_x^\infty L(x,x')M(x',t)\mathrm{d}x' - m(x,t)\int_0^x L(x,x')\frac{x'}{x}\mathrm{d}x'. \tag{22}$$

The second term on the right hand side of Eqn. 22 represents the formation of particles of mass x from larger particles breaking down, and the third term represents the fragmentation loss from the population of members of mass x. The presence of the term $\frac{x'}{x}$ in the final integral

ensures that the system conserves mass. The function $L(x, x')$ is the fragmentation kernel, and is analogous to the coagulation kernel, although it is not symmetric in its arguments (*i.e.*, with $x' < x$, particles of mass x' cannot form particles of mass x through fragmentation). For convenience, we write the full equation of a fragmentation-coagulation system in short as

$$\frac{\partial}{\partial t} m(x,t) = C(m) + F(m), \tag{23}$$

where we now write $m(x, t)$ is the number of floes of area x at time t.

The structure of Lensu's model (Eqns. 20, 21) corresponds to a pure fragmentation model with constant kernel $L(q, y) = 1$. It is shown in Lensu [1997] that this system admits the solution

$$G(p) = \exp\left(2 \int_0^1 q^p \beta(z) \mathrm{d}z t - 1\right), \tag{24}$$

$$N(t) = N_0 \exp(t) \tag{25}$$

where $G(p)$ is an integral transform:

$$G(p) = \int_0^1 x^p f(q) \mathrm{d}q.$$

Analysis of the solution as $t \to \infty$ reveals that the distribution of fragment sizes, f approaches a log-normal form Lensu [1997]. When either $F(m)$ or $C(m)$ is zero in Eqn. 23, the system does not display a stationary solution except in the trivial case when both are zero. It has been proved (Escobedo et al. [2005], Fournier and Laurenot [2005]) that a broad class of kernels admit self-similar solutions for both pure coagulation ($F(m) = 0$) and pure fragmentation ($C(m) = 0$) models, where a self-similar solution $u(x, t)$ can be written in terms of a scaling function $s(t)$:

$$m(x,t) = s^{-2}(t) v(x s^{-1}(t)). \tag{26}$$

Fragmentation functions of the form

$$b(y, y') = b_0(y)B(y'/y) \tag{27}$$

with

$$b_0(y) = y^{\beta} \tag{28}$$

$$\gamma \geq -1 \tag{29}$$

and $B(\cdot)$ is (effectively) a probability distribution defined on the interval $[0,\ 1]$ (as $y' < y$) were considered in Escobedo et al. [2005]. The model considered by Lensu in Lensu [1997] belongs to the class of models considered in Escobedo et al. [2005] with $\beta = -1$ in Eqn. 28, and the results in Escobedo et al. [2005] apply to Lensu's work.

Given that the fragmentation SCMs are well studied, and there are general results about their behaviour which apply to existing sea ice models, it is likely that there is further value in the use of SCMs in modelling sea ice fracture processes, both as tools for modelling, and as conceptual objects used to further our understanding of the processes at work, and the distributions they generate.

7. Discussion and Conclusions

The SCM provides a powerful framework to address many open questions in sea ice modelling. The simplicity of the SCM allows the study of a wide variety of parameterisations of coagulation and fragmentation processes without creating strong demands on processor time, and the conceptual clarity of the SCM makes it a useful tool in studying sea ice redistribution. The robust presence of exponential and quasi-exponential populations produced by models with

a wide variety of rate kernels, suggests that the description of the redistribution process given by the SCM is sufficient for the production of ice thickness populations which are qualitatively similar to those observed. Clearly, the implementation of a SCM formulation in sea ice thickness distribution modelling in anything other than an idealised context must be adjusted to best represent the physical realities of the system under study. In the types of models we have considered, the ridging events are viewed as analogous to the interaction of two particles in the SCM. The 'block-stacking' representation of ridging is an over-simplification, but the coagulation model formalism provides a useful idealised framework for the study of the interplay between mechanical and thermodynamic process in sea ice.

As can be inferred from the analytic solutions of the SCM, exponential and quasi-exponential distributions arise naturally as a feature of the equations over a broad range of kernel specifications. That said, the rate kernels for which analytic solutions exist are not suited for sea ice modelling, particularly as the additive and multiplicative kernels model systems in which larger particles interact *more* frequently than smaller ones. While the constant kernel, $K = 1$, considered by Thorndike, is too simple to be a representation of the physical reality of ridging, it is at least not manifestly unphysical. Numerical simulations with a variety of rate kernels demonstrate that the quasi-exponential tails arise even in the case where these kernels do not admit analytic solutions.

While the thermodynamic term in our model is orders of magnitude smaller than the coagulation term for thick ice (as shown in Fig. 3) , our work nevertheless demonstrates the need for a balance between the thermodynamic forcing and the tendency of the ridging process to increase

ice thickness in an unchecked fashion Thorndike [2000]. A similar conclusion regarding the relationship between dynamics and thermodynamics is obtained in much more detail in Bitz and Roe [2004], using a viscous-plastic basin-scale model. There may be value in the use of simple coagulation models to further explore this aspect of sea ice models, as SCMs have been studied extensively and there is an extensive body of literature on their behaviour. With a firm understanding of the behaviour of both the thermodynamic and dynamic components of such a model, efforts could focus on the effect of their interaction on the population statistics.

Investigation of the model response to changes in the kernel intended to reflect the differences between the processes of rafting and ridging has shown that the model is only weakly sensitive to this aspect of its construction. Future work on this aspect of the model involves simulations using kernels which represent the rafting process as being more distinct from ridging redistributions. Model response to changes in the representation of rafting is important when studying the state of the thickness distribution of ice populations in scenarios which are dominated by rafting, such as are likely to occur in a future with a stronger melt season. By modifying the thermodynamic component of the model to represent predicted conditions, the model could be used to study the potential changes in the ice thickness distribution which would occur in a population dominated by rafting-type redistributions.

While it is beyond the scope of the present work, the models developed in this paper would be of greater utility and practical application with the relation of their components to measurable quantities of the ice pack. While we have shown that the exact specification of the kernel is not of primary importance in determining the shape of the thickness distribution, in order to use

the model to predict the behaviour of populations of ice, the approximate maximum magnitude of the kernel must be related to observed redistribution rates in ice. To obtain data-based estimates of the coagulation kernel one avenue might be to examine time series of satellite imagery, in order to estimate the rate of ridge formation. By complimenting this data with measurements of thickness distributions from the same area, either gathered using ice profiling sonar or by direct field measurements, $K(h, h')$ could potentially be suitably constrained. Another method which could be used is the tuning of the SCM-based model using the output of a small-scale ice dynamical model, such as those developed by Hopkins Hopkins [1998] to estimate rates of ridge formation and their thickness dependence.

In addition to our examination of the coagulation model, we have compared the related fragmentation model with work on sea ice floe size distribution, and shown that work done by Lensu Lensu [1997] is a form of fragmentation model for which the mathematical properties are understood, and which display many of the features we seek in a model of the floe size distribution. The derivation of a model which we have shown to be mathematically equivalent to a fragmentation model in the literature, coupled with the known mathematical properties of this type of system suggest that further investigation of fragmentation models could be valuable.

The persistent presence in sea ice populations of clear statistical features, such as the exponential tail of the thickness distribution and the log-normality of floe size distribution, begs the question of the processes leading to these properties. It is known that the detailed dynamic interactions which drive the evolution of the population are complex due to the nature of the material. As we have shown, the SCM formalism (appropriately augmented with terms rep-

resenting thermodynamic processes and the formation of open water) presents an appealingly simple and robust tool which may provide a deeper understanding of the processes which drive the statistics of sea ice populations. In Godlovitch et al. [2011] we develop a model of sea ice thickness distribution dynamics which treats redistribution in a similar fashion to the models explored in this work, but which features redistribution processes directly informed by our understanding of the physical properties of sea ice, and its observed redistribution behaviour.

Appendix: Examples of SCMs with Exact Solutions

The existence of analytic solutions to some SCMs increases their appeal as a modelling tool. Study of the analytic solutions of SCMs can yield insight into the behaviour which may be produced in a model which includes an SCM component. When $K(j,k) = 1$, the discrete SCM (Eqn. 1) has the solution

$$u_k(t) = \left(1 + \frac{t}{2}\right)^{-2} \left(\frac{t}{2+t}\right)^{k-1}. \tag{30}$$

For the linear rate kernel, $K(j,k) = j + k$, the solution to the discrete system is of the form

$$u_k(t) = e^{-t} B(1 - e^{-t}, k), \tag{31}$$

where $B(t,x)$ is the Borel distribution:

$$B(t,x) = \frac{(tx)^{x-1} e^{-tx}}{x!}. \tag{32}$$

When $K(k,j) \propto kj$, the solution in the discrete case is given by

$$u_k(t) = i^{-1} B(t,k), \tag{33}$$

where $B(t,k)$ is the Borel distribution again.

For the constant kernel, the solution to the continuous equations (Eqn. 2) is $u(x,t) = 4t^{-2} e^{-2x/t}$.

When the kernel is a linear function, the continuous system has the solution

$$u(x,t) = \frac{1}{\sqrt{2\pi}} e^{-t} x^{-3/2} e^{e^{-2t}x/2}. \tag{34}$$

Finally, the continuous system with multiplicative kernel, $K(x,y)$, has the solution

$$u(x,t) = (2\pi)^{-1/2} x^{-5/2} e^{-t^2 x/2} \tag{35}$$

The solution to the SCM with multiplicative kernel (Eqn. 33) can become unbounded in finite time under certain conditions. The solutions to the SCM with constant and additive kernels are bounded for all time, and they conserve the total size of the system ($\sum_{k=0}^{\infty} k u_k(t)$, $\int_0^{\infty} x u(x,t) \mathrm{d}x$) for all time *viz.*, Shirvani and Roessel [1992].

References

552 Aldous, D. J., 1999. Deterministic and stochastic models for coalescence (aggregation and co-
553 agulation): a review of the mean-field theory for probabilists. Bernoulli 5 (1), 3–48.

554 Bitz, C. M., Holland, M. M., Weaver, A. J., Eby, M., 2001. Simulating the ice-thickness distri-
555 bution in a coupled climate model. Journal of geophysical research 106 (C2), 2441–2463.

556 Bitz, C. M., Roe, G. H., 2004. A mechanism for the high rate of sea ice thinning in the arctic
557 ocean. Journal of Climate 17 (18), 3623–3632.

558 Escobedo, M., Mischler, S., Ricard, M. R., 2005. On self-similarity and stationary problem
559 for fragmentation and coagulation models. In: Annales de l'Institut Henri Poincare (C) Non
560 Linear Analysis. Vol. 22, 99–125.

561 Feltham, D. L., 2008. Sea ice rheology. Annual Review Of Fluid Mechanics 40, 91–112.

562 Flato,G., Hibler, W., 1995. Ridging and strength in modeling the thickness distribution of Arctic
563 sea ice. Journal of Geophysical Research 100 (C9), 18611–18626.

564 Fournier, N., Laurenot, P., 2005. Existence of self-similar solutions to smoluchowski's coagu-
565 lation equation. Communications in Mathematical Physics 256 (3), 589–609.

566 Frenklach, M., 1985. Dynamics of discrete distribution for smoluchowski coagulation model.
567 Journal of colloid and interface science 108 (1), 237–242.

568 Godlovitch, D.,Flato,G.,Monahan,A.,2011. A Stochastic Model Of Sea Ice Thickness Dynam-
569 ics. Cold Regions Science and Technology, accepted with revisions.

570 Hammond,A.,Rezakhanlou,F.,2007.The Kinetic Limit of a System of Coagulating Brownian
571 Particles.Archive for Rational Mechanics and Analysis 185 (1), 1–67.

572 Hibler, W. D., 1979. A dynamic thermodynamic sea ice model. Journal of Physical Oceanogra-
573 phy 9 (4), 815–846.

574 Hibler, W. D., 1980. Modeling a variable thickness sea ice cover. Monthly weather review
575 108 (12), 1943–1973.

576 Hibler, W. D., 2001. Sea ice fracturing on the large scale. Engineering Fracture Mechanics
577 68 (17-18), 2013–2043.

578 Holland, M. M., Bitz, C. M., Hunke, E. C., Lipscomb, W. H., Schramm, J. L., 2006. Influence
579 of the sea ice thickness distribution on polar climate in CCSM3. Journal of Climate 19 (11),
580 2398–2414.

581 Hopkins, M., 1998. Four stages of pressure ridging.Journal of Geophysical Research 103 (C10),
582 21883–21891.

583 Mark A. Hopkins and Alan S. Thorndike, *Floe formation in arctic sea ice*, Journal of Geophys-
584 ical Research **111** (2006), 9 PP.

585 Hunke, E. C., Dukowicz, J. K., 1997. An elastic-viscous-plastic model for sea ice dynamics.
586 Journal of Physical Oceanography 27 (9), 1849–1867.

587 Lensu, M., 1997. Correlations between fragment sizes in sequential fragmentation. Journal of
588 Physics A: Mathematical and General 30, 7501.

589 Lensu, M., 2003. The evolution of ridged ice fields. Ph.D. thesis, Helsinki University of Tech-
590 nology. http://lib.tkk.fi/Diss/2003/isbn9512265591/isbn9512265591.pdf, 142 PP.

591 Maykut, G. A., Untersteiner, N., 1971. Some results from a time-dependent thermodynamic
592 model of sea ice. Journal of Geophysical Research 76 (6), 1550–1575.

593 Palmer, A. C., Sanderson, T. J. O., 1991. Fractal crushing of ice and brittle solids. Proceedings:
594 Mathematical and Physical Sciences 433 (1889), 469–477.

595 Rothrock, D. A., Thorndike, A. S., 1984. Measuring the sea ice floe size distribution. Journal of
596 Geophysical Research 89 (C4), 6477–6486.

Sanderson, T. J. O., 1988. Ice mechanics: Risks to offshore structures. Kluwer Academic Publishers, Norwell, MA. ISBN 9780860107859. 253 PP.

Shirvani, M., Roessel, H., 1992. The mass-conserving solutions of Smoluchowski's coagulation equation: The general bilinear kernel. ZAMP Zeitschrift fur angewandte Mathematik und Physik 43 (3), 526–535.

Thorndike, A., 2000. Sea ice thickness as a stochastic process. Journal of Geophysical Research 105 (C1), 1311–1313.

Turcotte, D. L., 1986. Fractals and fragmentation. Journal of Geophysical Research 91 (B2), 1921–1926.

Wadhams, P., 1983. Sea ice thickness distribution in fram strait. Nature 305 (5930), 108–111.

Wadhams, P., 1987. Sea ice thickness distribution in the greenland sea and eurasian basin, may 1987. Journal of Geophysical Research-Oceans 97 (C4), 13933–14346 .

Wadhams, P., Davy, T., 1986. On the spacing and draft distributions for pressure ridge keels. J. Geophys. Res 91 (C9), 10697–10708.

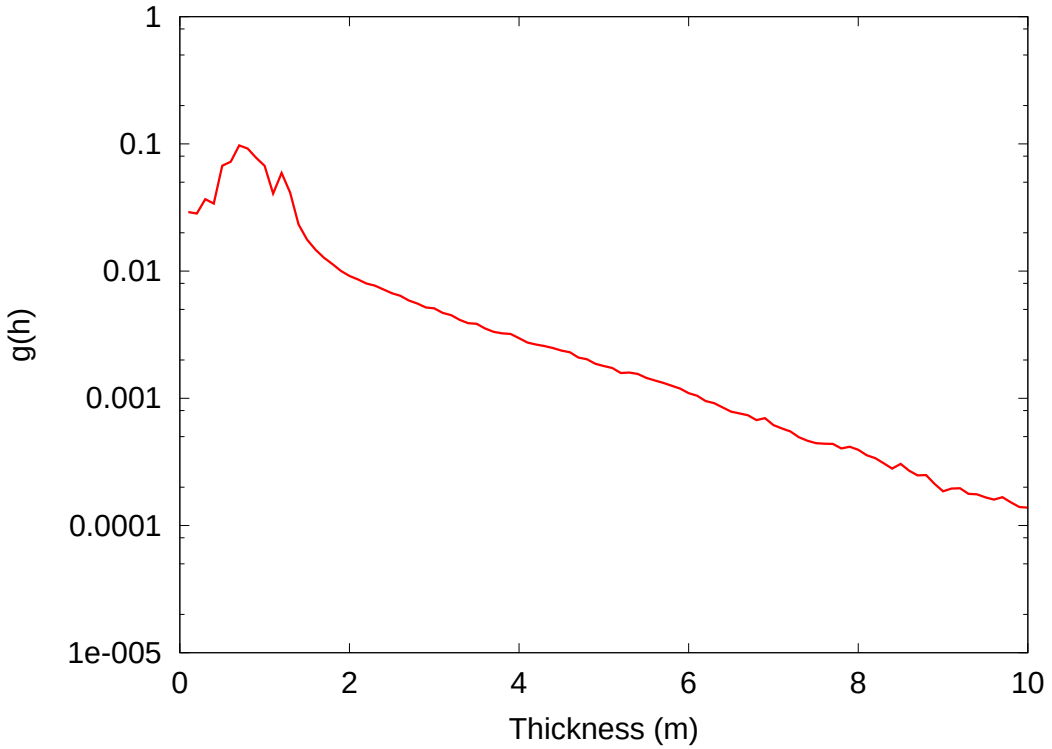

Figure 1. Empirical mean thickness distribution, $g_\mu(h)$ generated from sonar measurements of ice thickness in January in the Beaufort Sea over the period 1990-2002

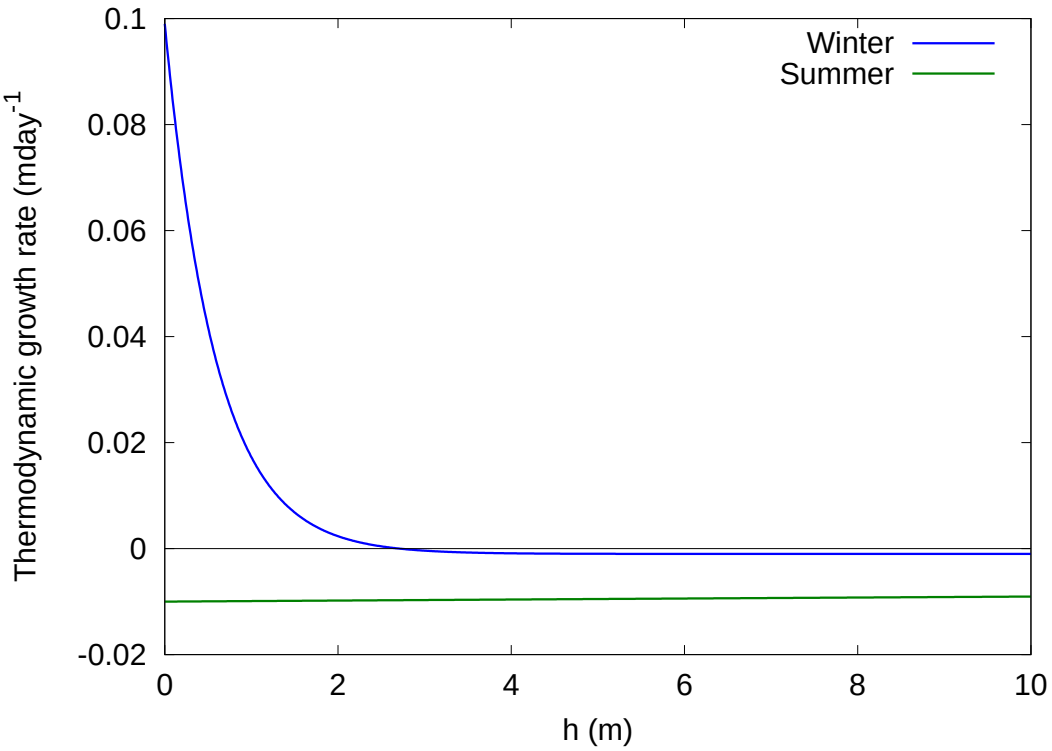

Figure 2. Summer and winter growth and melt rates for ice from Maykut Maykut and Untersteiner [1971]

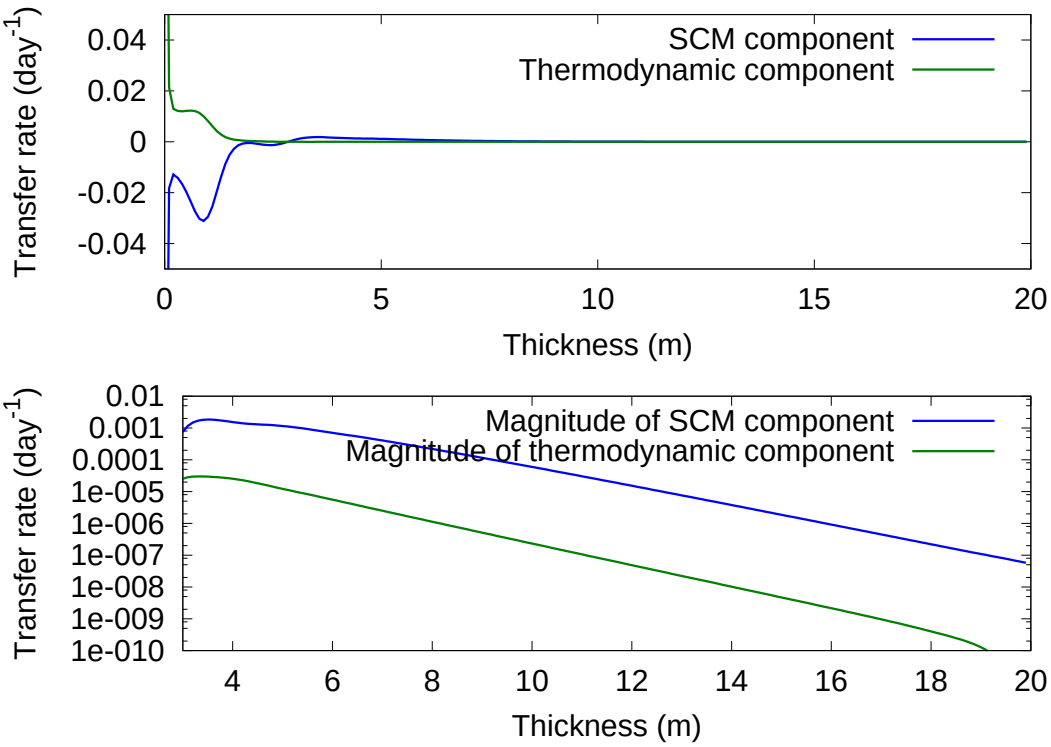

Figure 3. Magnitudes of the SCM terms and thermodynamic term in Eqn. 15 with an exponential kernel at the final timestep of the simulation displayed in the top left quadrant of Fig.4

Table 1. Rate kernels for coagulation model, with scaling constant r (note that r takes different values for each kernel)

Run Number	Kernel $K(x, y)$
1	r
2	$r\exp^{-\beta(x+y)}$
3	$r(xy)$
4	$r(x+y)$

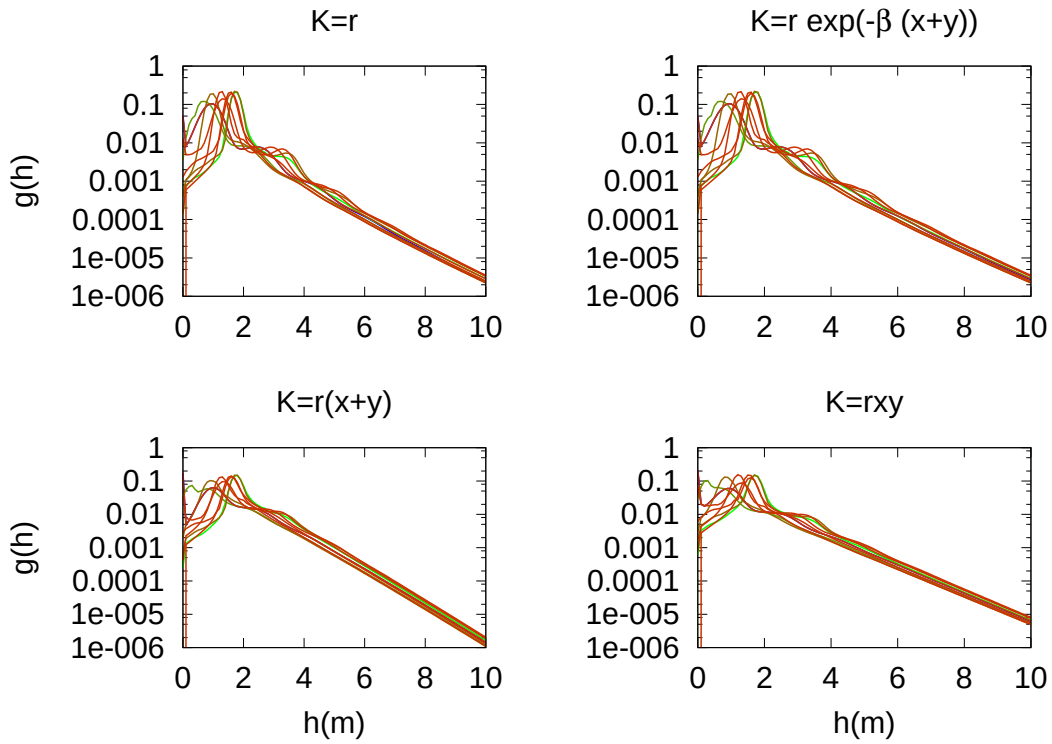

Figure 4. Coagulation model with kernels from Table 1. Population is plotted every 200 days from runs of 2000 days, with color changing from green to red with increasing t.

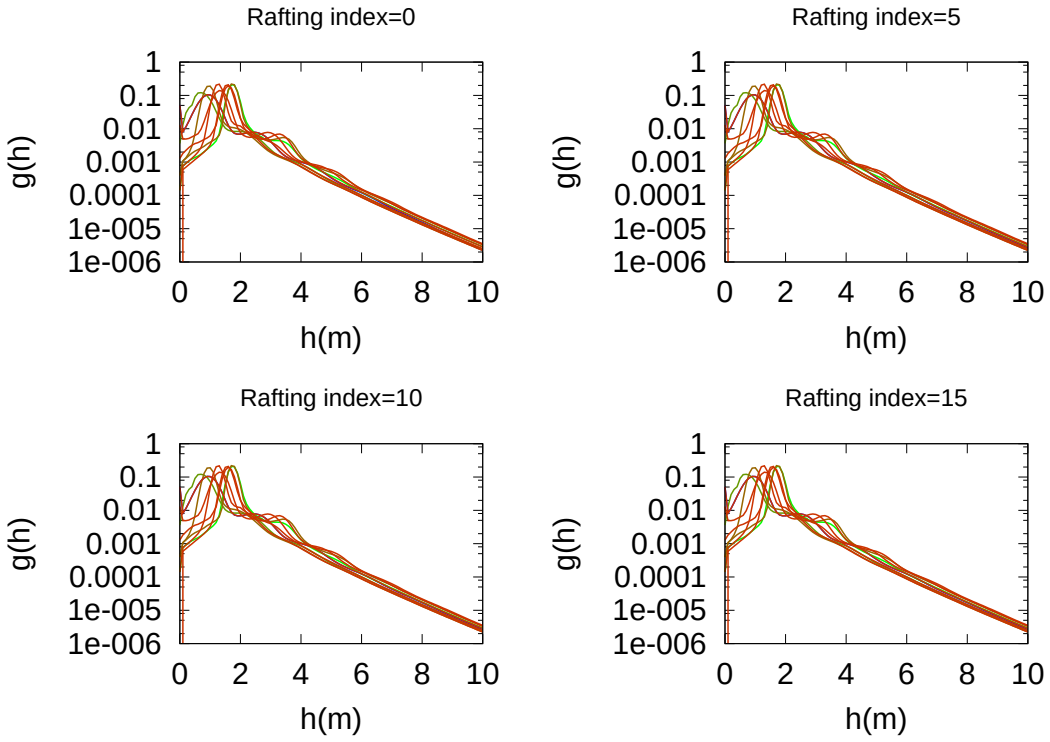

Figure 5. Coagulation model runs using a piecewise constant coagulation kernel with varying rafting cutoff indices as indicated. Rafting ice has kernel $K = 4$, ice above the rafting cutoff has $K = 1$. Timing and colouring as in Fig.4

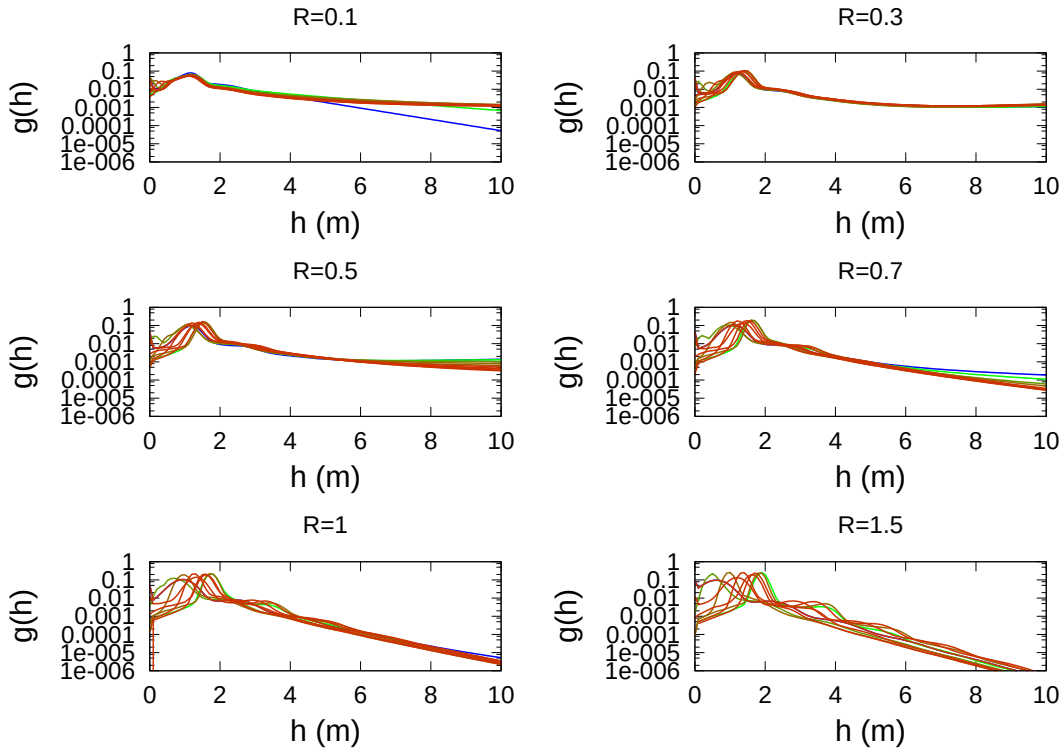

Figure 6. Coagulation model runs with varying relative strengths of thermodynamic and dynamic components. Snapshots of population taken every 2000 timesteps for 20000 timesteps, with the initial curve pure blue, and the final curve pure red.

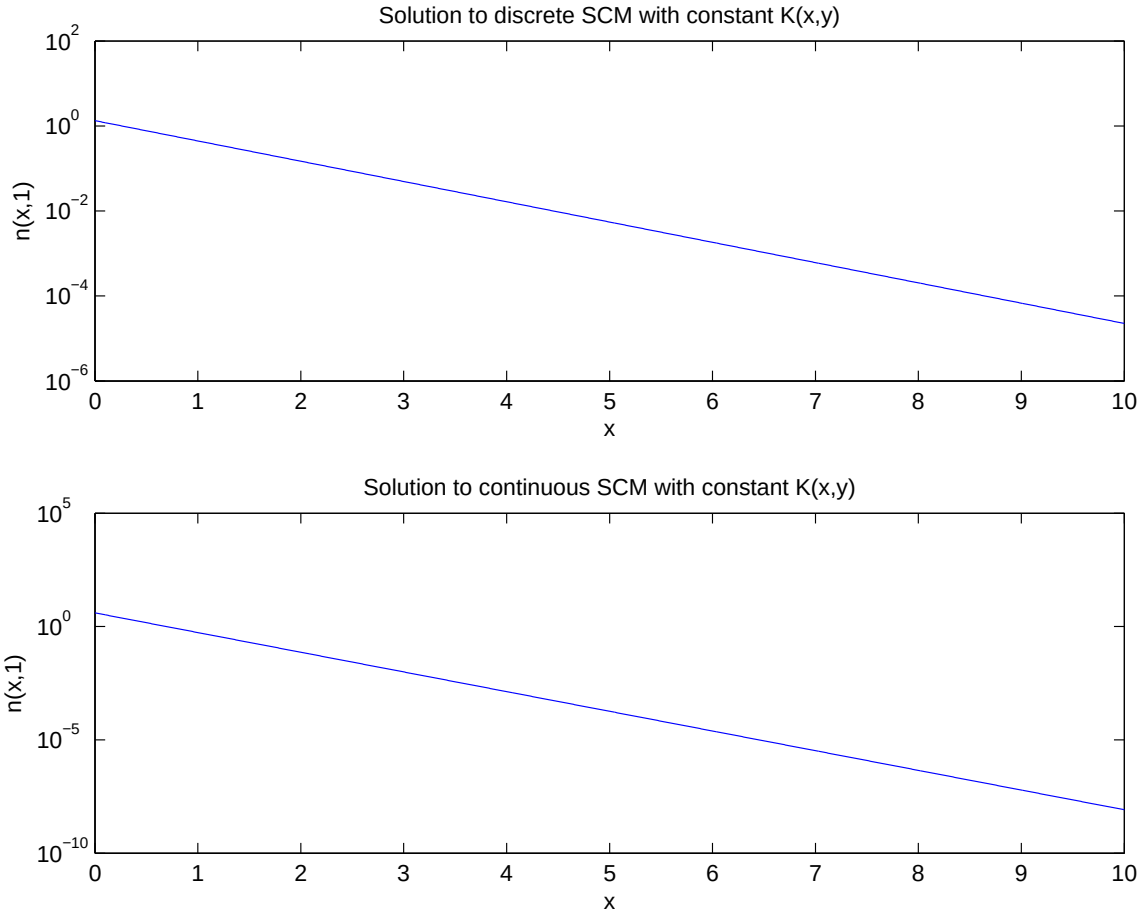

Figure 7. Solutions to SCM with $K(j,k) = 1$

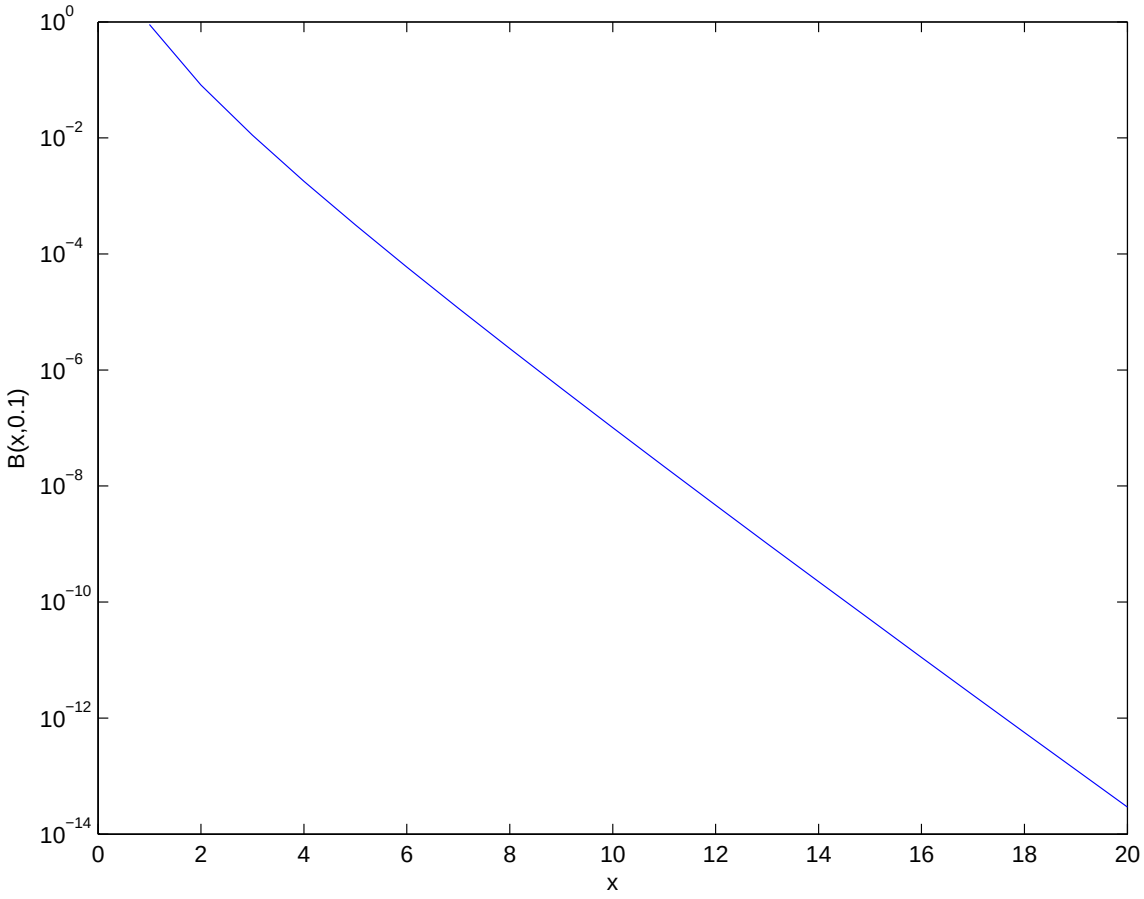

Figure 8. The Borel distribution with $t = 0.1$